Surface displacement detection using object-based image analysis, Tashkent region, Uzbekistan

M Juliev[1,2*], *W* Ng[3], *I* Mondal[4], *D* Begimkulov[5], *L* Gafurova[6], *M* Hakimova[7], *O* Ergasheva[6] and M Saidova[5]

[1]"Tashkent Institute of Irrigation and Agricultural Mechanization Engineers" National Research University, Kory Niyoziy str., 39,100000 Tashkent, Uzbekistan
[2]Turin Polytechnic University in Tashkent, Little Ring Road Street 17, 100095 Tashkent, Uzbekistan
[3]Earth Observation Data Centre (EODC) for Water Resources Monitoring GmbH, Franz-Grill-Straße 9, 1030 Vienna, Austria
[4]Indian Institute of Engineering Science and Technology, Shibpur-711103 India
[5]Tashkent State Technical University, University Street 2, 100095 Tashkent, Uzbekistan
[6]National University of Uzbekistan, University street 4, 100174 Tashkent, Uzbekistan
[7]Karshi engineering economics institute, Mustakillik street 225, 180100 Karshi, Uzbekistan

Abstract. Landslides can be listed as a major natural hazard for the Bostanlik district, Uzbekistan characterized by its mountain terrain. Currently, a monitoring system is not in place, which can mitigate the numerous negative effects of landslides. The current study presents the first Earth Observation-based landslide inventory for Uzbekistan. We applied a random forest Object-Based Image Analysis (OBIA) on very high-resolution GeoEye-1 Earth observation data to detect surface displacement. While performing 10-fold cross-validation to assess the classification accuracy. Our results indicate very high overall accuracy (0.93) and user's (0.87) and producer's (0.91) accuracy for the surface displacement class. We determined that 5.5% of the study area was classified as surface displacement. The obtained results are highly valuable for local authorities for the management of landslides, hazard prevention, and land use planning.

1 Introduction

Landslides, also referred to as surface displacements, are prominent natural hazards, which can be catastrophic to economic activities (i.e. damage to property and infrastructure) and human health (i.e. causing death and injuries) and are affecting many countries around the world [1]. A landslide is the spatial disposition of sedimentation and weathering areas of gravity-induced mass movement processes [2]. Accordingly, landslide detection and the application of countermeasures are significant tools for mountain risk engineers [3]. Landslide inventory maps should be prepared to know the landslide type, volume, and year of occurrence. Furthermore, a historical landslides inventory is important for the analysis of

* Corresponding author: mukhiddinjuliev@gmail.com

© The Authors, published by EDP Sciences. This is an open access article distributed under the terms of the Creative Commons Attribution License 4.0 (https://creativecommons.org/licenses/by/4.0/).

pre- and post-disaster studies [4]. Likewise. Landslide susceptibility and landslide risk mapping require accurate landslide inventory maps [5–8].

Apart from other natural hazards, the territory of Uzbekistan is prone to landslides. Over the past 80 years >2,600 landslide events were documented [9–12]. Around 65% of all landslides in Uzbekistan are located in the Tashkent region. The Bostanlik district tops the list where most of the landslide events occurred which were triggered by earthquakes, snowmelt, or precipitation. The Charvak mountain reservoir is especially susceptible to landslide occurrences, in particular near the water body. Therefore, monitoring of landslides is essential, and studies like landslide susceptibility and risk mapping can help to mitigate and prevent the consequences of natural hazards [5,13].

Earth Observation (EO) is widely utilized in environmental sciences, but only during the last decade introduced to landslide studies [14]. EO datasets are essential to acquire reliable information for high altitude areas without the need for extensive and tedious fieldwork. Advanced EO approaches to produce effective results in the field he landslide detection, mapping, and analysis. The optical very high-resolution (VHR) EO satellites (i.e. WorldView, GeoEye-1) have proven to be very successful for detailed landslide inventory mapping [7,15,16].

Aerial photos or satellite images with in situ observations are used to prepare landslide inventory maps. Visual interpretation of landslides is a time-consuming task therefore researchers developed automated landslide detection methods [17]. Different methods used for the automated detection of landslides consist of pixel-based and object-based approaches. Object-based image analysis methods (OBIA) were proposed for landslide and surface displacement mapping by several researchers [11, 25-28, 8]. OBIA is a tool for the semi-automatically representation and classification of surface displacement processes, utilizing mostly high-resolution satellite datasets. The main concept of OBIA consists of segmentation and classification of subsequential segments. This method has proven to be effective for landslide mapping and landslide inventories [27]. Hölbling et al. [18] applied an OBIA method for landslide mapping in five areas in Austria and Italy using satellite imageries of Landsat 7, SPOT-5, WorldView-2/3, and Sentinel-2. The objectives of the paper were to compare manual landslide mapping results to automated results. They describe advantages and disadvantages and report on similar results between the manual and automated classification. Feizizadeh et al. [19] employed OBIA for landslide delineation and landslide change detection using temporal data from the IRS-1D, SPOT-5, and ALOS sensors in northern Iran. The authors generated landslide maps for 2005 and 2011 with accuracies of 0.93 and 0.94 respectively and acknowledged the potential of OBIA for surface displacement delineation.

The main scope of the present study is to perform OBIA for surface displacement detection for the surrounding area of the Charvak Reservoir an important site in the Bostanlik district, Tashkent region, Uzbekistan. This work is the first attempt of performing an automated surface displacement or landslide inventory using EO data within the territory of Uzbekistan. The main objectives can be summarized as follows:

- utilizing very high resolution GeoEye1 for the classification;
- verifying the suitability of OBIA for the land cover classification and surface displacement;
- obtaining detailed surface displacement areas for the study area for further utilizing them for landslide susceptibility and risk mapping.

2 Study area

The Bostanlik district is located in the north-eastern part of Uzbekistan between 41°00' and 42°20' North and 69°30' and 71°20' East (Figure 1). The study area measures 4,982 km2

and is the largest district in the Tashkent region. The study focuses on a subset of the surrounding of the Charvak reservoir for the area of 307 km2 with Gazalkent as the administrative center. According to the census of 2013 [20,21], about 160,000 people inhabited the area with more than 60% of the residents living in rural areas.

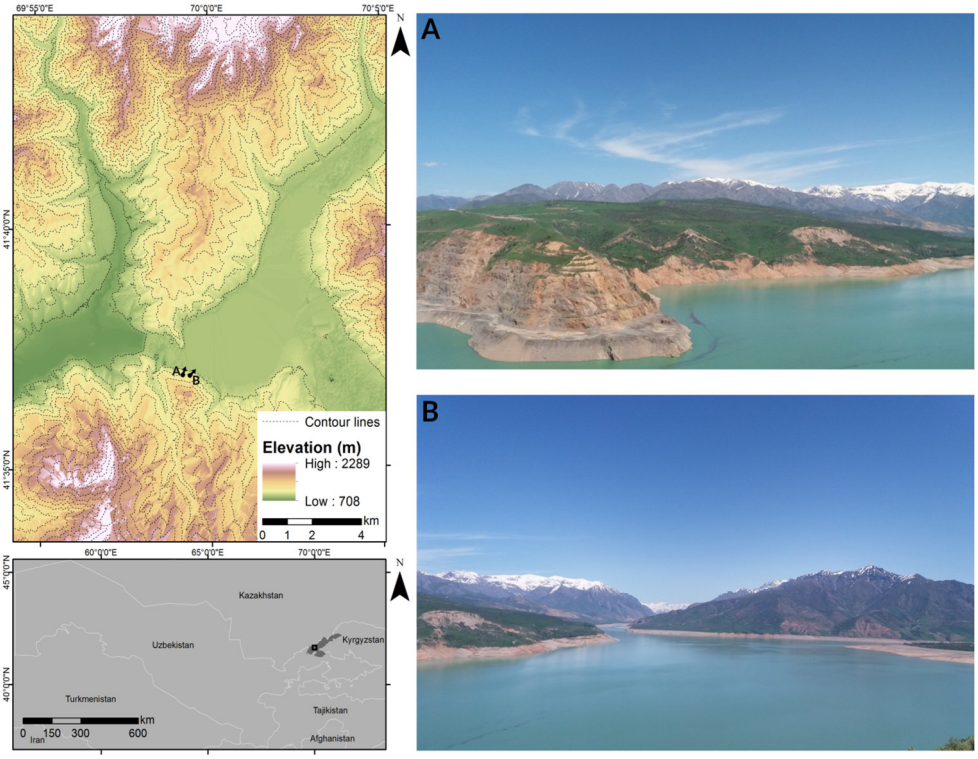

Fig. 1. The study area is located in the Bostanlik district of Tashkent region, Uzbekistan, displayed with contour lines and a digital elevation model (SRTM). A and B are photos taken during the field mission in northern (A) and northeastern (B) directions showing surface displacements.

The study area, mostly covered by quaternary loess deposits, is vulnerable to erosion and landslide processes. The area includes high mountains such as the Western Tien Shan, Karzhantau, Pskem, Ugam, and Chatkal. The elevation varies from 568 m to 4,301 m a.s.l. (summit of Mt. Adelung). Elevation generally increases from west to east and from south to north. The district further belongs to a seismically active zone, resulting in an average occurrence of eight earthquakes per year [22].

The area is further characterized by a continental climate: annual mean minimum and maximum, and absolute minimum and maximum temperatures are -9°C, +21°C, -26°C and +46°C, respectively. The total amount of precipitation obtained from metro stations reaches up to 800–1200 mm per year and the main drainage system of the area is the Chirchik River. Within the district, the Charvak Reservoir covers an area of 40 km2 and stores two billion m3 of water [20].

3 Metodology

The study area was visited in July 2018 and an extensive set of landslides were cataloged and digitized (n=45). Land cover classes were interpreted through a combination of Google Earth orthophoto and the GeoEye-1 interpretation. In total, 15 land cover classes were

selected and trained in a random forest (RF) model these are displayed in Table 1, including the number of segments assigned for training. To select reference data for the surface displacement segments, the digitized reference polygons were overlaid with the matching segmentation. The remaining numbers of land cover classes were trained by matching representative segments to *in situ* collected data, complemented with orthophoto interpretation. Due to the small number of data collected in the field we assigned on average 39 training polygons per class.

Table 1. Description of the land cover classes and several reference polygons for training the random forest model.

Class	**Description**	**Ref. data**
Surface displacement	Debris flows, landslides, erosion processes	58
Bedrock	Exposed outcrops of the rocky material	34
Bare soil	Areas of exposed soil and barren fields	37
Fallow fields	Agriculture parcels without any crops	21
Low-intensity agriculture (LIA)	Areas with the sparse crops	39
High-intensity agriculture (HIA)	Parcels with the dense crops	26
Meadows	Areas covered by grass and other non-woody plants	30
Shrub land	Areas covered by bushes, shrubs including grasses, herbs	49
Sparse forest	Areas covered with sparse tall trees cover	40
Dense forest	Areas covered with the dense and tall trees	37
Shadows	Shadows from the bedrock, residential and forested areas	43
Water	Water bodies and rivers	Mask
Unpaved roads	Roads made from native material e.g., gravel	32
Paved roads	Roads covered with the asphalt	40
Built-up	Residential, commercial, and industrial buildings	56

GeoEye-1 is a commercial very high-resolution satellite operated by Digital Globe established in 2009. The sensor collected data in four multi-spectral channels (red, green, blue, and near-infrared) at 2m spatial resolution and one panchromatic channel at 0.5-meter spatial resolution. The Digital Globe Foundation provided a data set of the study area acquired on 15 July 2016. The data were atmospherically and topographically corrected using 606 reference polygons. A water mask was created from the green and Near Infra-Red (NIR) spectral bands, to remove the water bodies using an empirically selected threshold of normalized difference water index (NDWI, eq. 1) proposed by McFeeters [23].

$$NDWI = \frac{green-nir}{green+nir} \quad (1)$$

Aster global digital elevation map version 2 (GDEM V2) data with a spatial resolution of 1 arc-second was acquired through the Earth Explorer portal operated by the U.S. Geological Survey (USGS) Earth Resources Observation and Science (EROS) Center. This dataset provides the highest possible spatial resolution, which is open-source, and available for the study area. The GDEM V2 was resampled to match the spatial resolution of the GeoEye1 data and used to calculate slope and aspect using ArcGIS.

The pre-processed GeoEye-1 data was used to calculate both the normalized difference vegetation index (NDVI, eq. 2) and green ratio (GR, eq. 3) [24].

$$NDVI = \frac{nir-red}{nir+red} \quad (2)$$

$$GR = \frac{green}{red} \quad (3)$$

In addition, the VHR satellite data was used to generate texture information. Toscani et al. [25] proved an increase in classification accuracy when including coiflets) a member of the wavelet family the feature stacks. Wavelet Toolbox in MATLAB for spectral bands to produce the mean of horizontal (H), vertical (V), and diagonal (D) detail coefficients.

For each of the 26 input features (i.e. spectral bands, coiflets, vegetation indices, elevation, slope, and aspect) statistical features (n=12) were calculated per object (i.e. mean, standard deviation, and percentiles). In total 312 input features were assessed to build the RF model. We assessed the RF model with a large number of features, through the Mean Decreasing Accuracy (MDA) after which we identified features that contribute to the model accuracy while excluding underperforming features, thus creating a robust and optimized model.

VHR EO data is highly suitable for an object-based approach (OBIA) and many authors report improved accuracy [26]. OBIA has the advantage of i) significantly increasing the number of input features to train the model as information (i.e. statistics) can be extracted from an object, and ii) removing the "salt and pepper" effect often encountered in pixel-based approaches. Therefore, we implemented a segmentation to find meaningful objects representing the land cover classes found in the study area. We applied the Large Scale Mean Shift (LSMS) segmentation provided by Michel et al. [27] implemented in the open-source software OTB version 5.4.0 in R version 3.5 as it provides an open-source solution to create high-quality segmentation results and does not require a priori knowledge. This non-parametric density-based clustering algorithm requires three parameters: (a) Spatial Radius (spatial distance); (b) Range Radius (spectral difference); and (c) Minimum Size (merging criterion). These criteria were used to group pixels together into the cluster by assessing neighboring pixels whose range distance is below the range radius (and optionally spatial distance below spatial radius). We used the atmospherically corrected GeoEye1 data (bands: NIR, Red, Green, and Blue) and empirically assessed the parametrization until representative polygons were produced matching reference polygons recoded during the field mission.

Random Forest is a well-established ensemble Machine Learning Algorithm used in a large number of object-based studies. Soil erosion and landslide detection using RF were done for several studies.

RF can be optimized, in terms of accuracy and processing time, by performing a parametrization process, therefore reducing the number of input features. The feature importance was calculated as Mean Decreasing Accuracy (MDA), which was generated within RF by running the model and systematically testing which features impact most the Out-Of-Bag (OOB) accuracy of the classification if left out. The MDA values were then used for feature ranking and selection, following approaches described by Genuer et al., Immitzer et al., and Ng et al. [29].

To compensate for the relatively small amount of high-quality reference data, we applied 10-fold cross-validation. The reference dataset was randomly split into partitions, and the RF model was performed ten times using different subsets of respective training (90%) and validation (10%) data. Therefore, we generated ten unique combinations, without repetition of validation polygons. The omitted polygons for validation were assessed by generating confusion matrices derived from the sum of the 10 classification

results Foody et al. [30], where after, standard statistical metrics were calculated including i)overall accuracy (OA): the total number of correctly classified polygons by the total number of reference polygons, ii) user's accuracy (UA): dividing the number of correctly classified polygons for each class by the total number of polygons that were classified in that class, iii) producer's accuracy: dividing the number of correctly classified polygons in each class (on the major diagonal) by the number of reference polygons of that class, and iv) Kappa: evaluates how well the classification performed as compared to just randomly assigning values.

4 Results and discussion

The confusion matrix derived from the 10-fold cross-validation (Table 2) displays very high User accuracy and Producer's accuracy for all classes. Confirming its suitability for detecting surface displacements (UA: 0.87 and PA: 0.91). The overall accuracy (0.93) and Kappa (0.92) of the random forest classification are in line with other published studies [18,19]. The mean decreases in accuracy (not shown) indicate that from the 312 input features the NDVI is most contributing to the accuracy, appearing ten times in the top 20 of best-scoring features. The 20th, 25th percentile, and mean are best performing statistical features, all of which appear three times in the top 20. The features derived from the ASTER GDEM (V2) did not appear in the final selection, which can be explained by the coarse spatial resolution.

Table 2. 10-fold cross-validation confusion matrix. The sum of the reference polygons is shown in the columns, while the sum of the classified polygons is shown in the rows.

	Bedrock	**Shadows**	**Dense forest**	**HIA**	**Paved roads**	**Unpaved roads**	**Fallow fields**	**LIA**	**Built-up**	**Shrub land**	**Sparse forest**	**Bare Soil**	**Meadows**	**Surface displacements**	**User's accuracy**
Bedrock	30	0	0	0	0	0	0	0	0	0	0	0	0	2	0.94
Shadows	0	29	0	0	0	0	0	0	1	0	0	0	0	0	0.97
Dense forest	0	0	36	1	0	0	0	0	0	0	1	0	0	0	0.95
HIA	0	0	0	25	0	0	0	1	0	0	0	0	0	0	0.96
Paved roads	0	0	0	0	38	0	0	0	1	0	0	2	0	0	0.93
Unpaved roads	0	0	0	0	0	29	0	0	0	0	0	0	0	1	0.97
Fallow fields	0	0	0	0	0	0	21	0	0	0	0	0	0	0	1.00
LIA	0	0	0	0	0	0	0	35	2	1	0	0	0	0	0.92
Built-up	1	0	0	0	2	0	0	1	52	0	0	2	0	0	0.90
Shrub land	0	0	0	0	0	0	0	0	0	47	1	0	0	0	0.98
Sparse forest	0	1	1	0	0	0	0	0	0	0	38	0	0	0	0.95
Bare Soil	2	0	0	0	0	0	0	0	0	0	0	31	0	1	0.91
Meadows	0	0	0	0	0	0	0	2	0	0	0	0	37	1	0.93
Surface displacements	1	0	0	0	0	3	0	0	0	1	0	2	1	53	0.87
Producer's accuracy	0.88	0.97	0.97	0.96	0.95	0.91	1.00	0.90	0.93	0.96	0.95	0.84	0.97	0.91	0.93

The land cover classification (Figure 3) corresponds to the in-situ observations. Among the 15 land cover classes shrub land, meadows, water, and sparse forest are dominant within the study area representing 28.37%, 18.22%, 11.31%, and 10.47% respectively (Table 3). Surface displacements were detected in 5,5% of the study area.

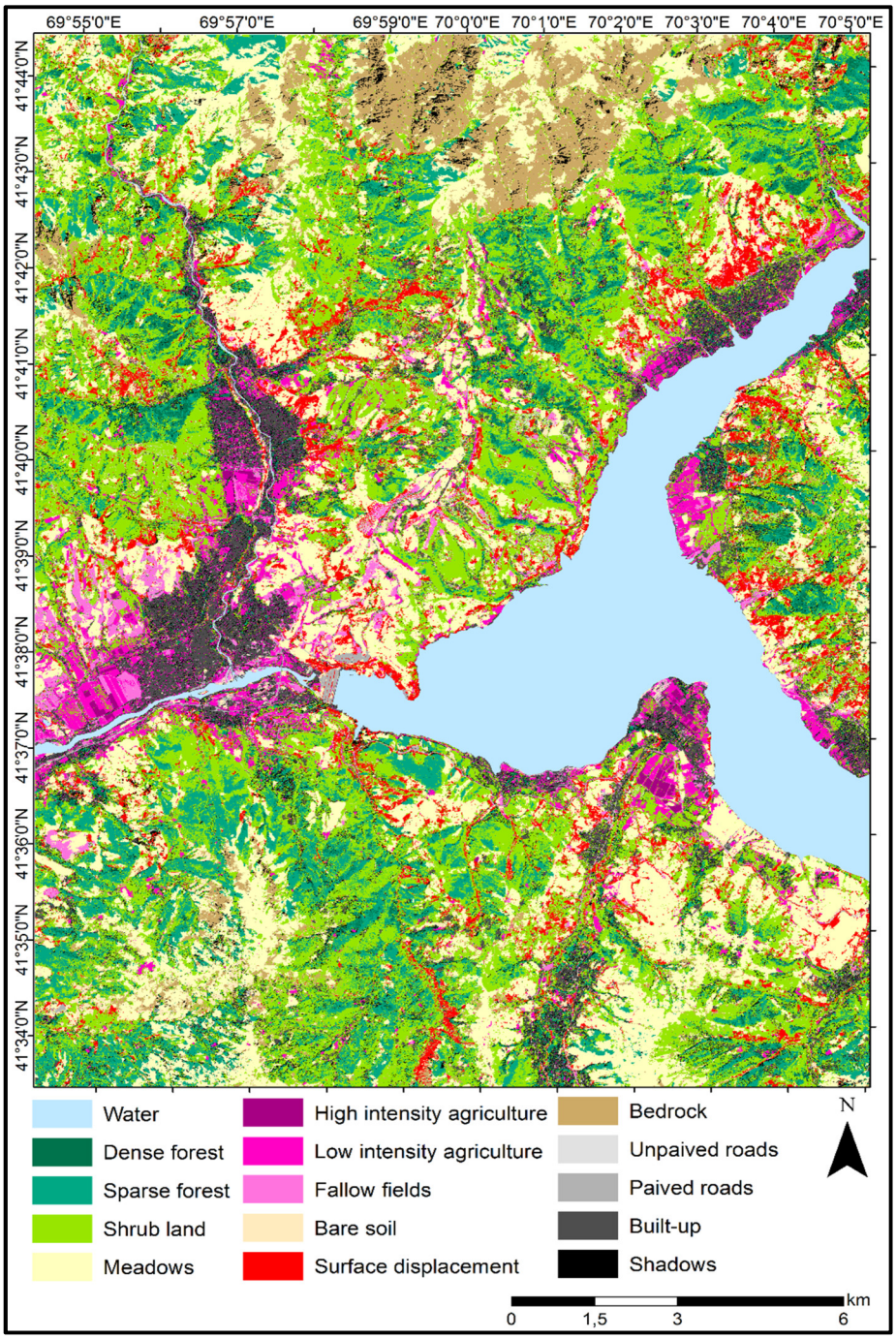

Fig. 2. Land cover map of the object-based random forest classification

Landslide monitoring is a difficult task within mountainous regions with high altitudinal ranges. Therefore, automated landslide inventories are needed for risk assessment pre- and post-disaster events [1]. As a highly landslide-prone area, the Bostanlik district is subjected to different types of landslides (e.g. translational slides, rotational slides, earth flows, debris flows, and debris slides), with various volumes [6,7]. An accurate landslide inventory is a preparatory step for a landslide susceptibility study. Manual landslide mapping is time-consuming and requires expertise, while automated detection provides rapid results with limited expert knowledge, which is especially valuable for crisis management.

Table 3. Individual class coverage in hectares and percentages

Class	**Area (ha)**	**Area (%)**
Surface displacement	1690.32	5.50%
Bedrock	1510.04	4.91%
Bare soil	506.13	1.65%
Fallow fields	445.41	1.45%
Low-intensity agriculture (LIA)	1234.75	4.02%
High-intensity agriculture (HIA)	182.41	0.59%
Meadows	5603.02	18.22%
Shrub land	8723.01	28.37%
Sparse forest	3221.13	10.47%
Dense forest	586.06	1.91%
Shadows	1097.84	3.57%
Water	3476.82	11.31%
Unpaved roads	458.38	1.49%
Paved roads	145.80	0.47%
Built-up	1871.39	6.09%

Most published EO-based landslide susceptibility maps apply pixel-based approaches [31]. The role of land classification study in the landslide is essential for determining the current scenario and for managing natural resources and environmental problems [32]. Our results demonstrate very high accuracy for surface displacement detection using OBIA. In line with Hölbling et al. [18] who compared manual and OBIA-based landslide detection methods for five study areas in the Alps using EO data with different spatial resolutions, achieving producers' accuracies from 0.70 to 0.95.

Figure 3 highlights the detected landslides, which were confirmed during the field mission. These surface displacements consist of different types of debris flows, landslides, and erosion processes. After a detailed analysis of the surface displacement class, we determined that the majority of the detected areas are deep-seated landslide bodies and shallow landslides (Figure 4). From the classification output, we can observe all deformations types, however for differentiating between landslide types expert knowledge and in situ observations are required.

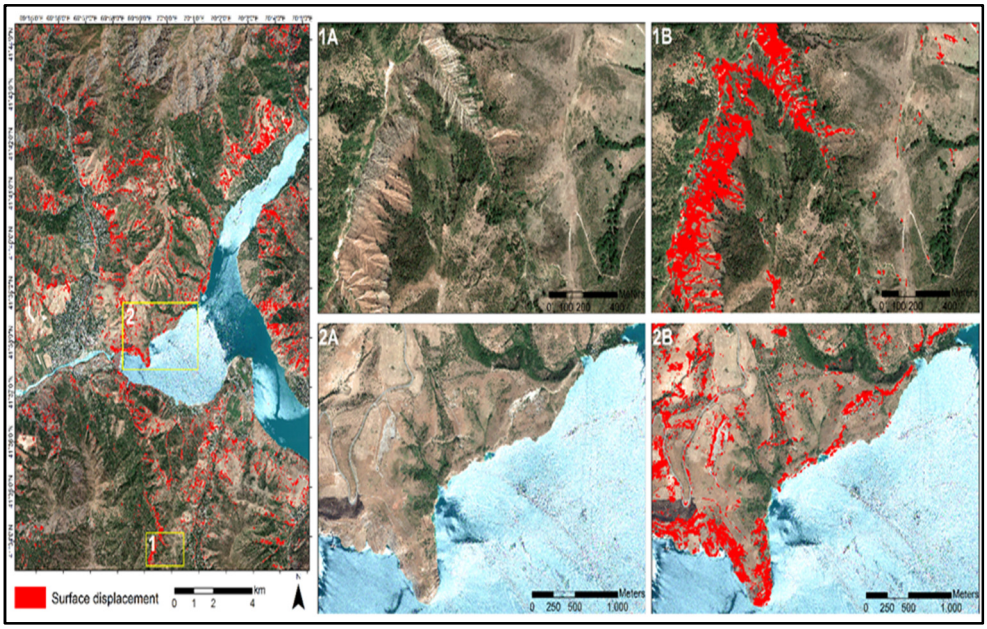

Fig. 3. Deep-seated landslide bodies and shallow landslides on the GeoEye1 EO data.

5 Conclusion

In this study, we present the first automated surface displacement map using OBIA and VHR GeoEye1 EO data for the Bostanlik district, Uzbekistan. We reported on the suitability of the method to obtain detailed surface displacement information for landslide susceptibility and risk mapping. Remote and isolated villages in high-altitude areas are especially vulnerable to surface displacements resulting in total cut-off from the outside world, obstructing rescue workers and aid efforts. Therefore, mapping landslide hotspots near such villages is vital. We conclude VHR optical sensors (i.e. GeoEye-1) and OBIA are providing highly accurate results for detecting surface displacements. The obtained result can be used and upscaled to a national level to create a detailed landslide inventory and can be combined with the existing manual maps.

In Uzbekistan there are two main agencies for landslide monitoring and forecasting: i) the State Service of the Republic of Uzbekistan on geological hazard monitoring from the State Committee of the Republic of Uzbekistan for Geology, and ii) the Mineral Resources and Ministry of Emergency Situations of the Republic of Uzbekistan. The results will be presented to these agencies for their large-scale implementation and regional research conducted with the cooperation of the local authorities.

References

1. J. Dou, K.T. Chang, S. Chen, A. Yunus, J.K. Liu, H. Xia, Z. Zhu, *Automatic Case-Based Reasoning Approach for Landslide Detection: Integration of Object-Oriented Image Analysis and a Genetic Algorithm*, J. Remote Sensing, **7,** 4318-42 (2015)
2. F. Guzzetti, A. Carrara, M. Cardinali, P. Reichenbach, *Landslide hazard evaluation: a review of current techniques and their application in a multi-scale study, Central Italy* J. Geomorphology**, 31,** 181-216 (1999)

3. F. Guzzetti, A.C. Mondini, M. Cardinali, F. Fiorucci, M. Santangelo, K-T Chang, *Landslide inventory maps: new tools for an old problem,* J. Earth-Science Reviews, **112,** 42-66 (2012)
4. A. Stumpf, N. Kerle, *Object-oriented mapping of landslides using Random Forests,* J. Remote Sensing of Environment, **115,** 2564-77 (2011)
5. M. Juliev, M. Mergili, I. Mondal, B. Nurtaev, A. Pulatov, J. Hübl, *Comparative analysis of statistical methods for landslide susceptibility mapping in the Bostanlik District, Uzbekistan,* J. Science of The Total Environment (2018)
6. Z. Chen, D. Song, M. Juliev, H. R Pourghasemi, *Landslide susceptibility mapping using statistical bivariate models and their hybrid with normalized spatial-correlated scale index and weighted calibrated landslide potential model,* J. Environ Earth Sci., **80,** 324 (2021)
7. I. Mondal, S. Thakur, M. Juliev, T. K. De, *Comparative analysis of forest canopy mapping methods for the Sundarban biosphere reserve, West Bengal, India,* J. Environ Dev Sustain, **23,** 15157-82 (2021)
8. I. Mondal, S. Thakur, M. Juliev, J. Bandyopadhyay, T.K. De, *Spatio-temporal modelling of shoreline migration in Sagar Island, West Bengal, India,* J. Coast Conserv, **24,** 50 (2020)
9. *Global Facility for Disaster Reduction and and Recovery (GFDRR),* Central Asia and Caucasus Disaster Risk Management Initiative (CAC DRMI) (2009)
10. M. Juliev, A. Pulatov, J. Hubl, *Natural hazards in mountain regions of Uzbekistan: A review of mass movement processes in Tashkent province,* Int. J. Scientific & Engineering Research**, 8**, 1102-8 (2017)
11. M. Juliev, A. Pulatov, S. Fuchs, J. Hübl, *Analysis of Land Use Land Cover Change Detection of Bostanlik District, Uzbekistan,* Polish J. Environmental Studies, **28**, 3235-42 (2019)
12. S. Khasanov, M. Juliev, U. Uzbekov, I. Aslanov, I. Agzamova, N. Normatova, S. Islamov, G. Goziev, S. Khodjaeva, N. Holov, *Landslides in Central Asia: a review of papers published in 2000–2020 with a particular focus on the importance of GIS and remote sensing techniques,* J. GeoScape, **15**, 134-45 (2021)
13. L. Gafurova, M. Juliev, *Soil Degradation Problems and Foreseen Solutions in Uzbekistan,* J. Regenerative Agriculture, ed D Dent and B Boincean (Cham: Springer International Publishing) 59-67 (2021)
14. T.R. Martha, N. Kerle, V. Jetten, C.J.V. Westen, K.V. Kumar, *Characterising spectral, spatial and morphometric properties of landslides for semi-automatic detection using object-oriented methods,* J. Geomorphology, **116**, 24-36 (2010)
15. D. Lu, P. Mausel, E. Brondízio, E. Moran, *Change detection techniques,* Int. J. Remote Sensing, **25,** 2365-401 (2004)
16. B. Alikhanov, M. Juliev, S. Alikhanova, I. Mondal, *Assessment of influencing factor method for delineation of groundwater potential zones with geospatial techniques. Case study of Bostanlik district, Uzbekistan*, J. Groundwater for Sustainable Development, **12,** 100548 (2021)
17. . Moosavi, A. Talebi, B. Shirmohammadi, *Producing a landslide inventory map using pixel-based and object-oriented approaches optimized by Taguchi method,* J. Geomorphology, **204,** 646-56 (2014)

18. D. Hölbling, C. Eisank, F. Albrecht, F. Vecchiotti, B. Friedl, E. Weinke, A. Kociu, *Comparing Manual and Semi-Automated Landslide Mapping Based on Optical Satellite Images from Different Sensors,* J. Geosciences**, 7,** 37 (2017)
19. B. Feizizadeh, T. Blaschke, D. Tiede, M. H. R. Moghaddam, *Evaluating fuzzy operators of an object-based image analysis for detecting landslides and their changes,* J. Geomorphology, **293**, 240-54 (2017)
20. I.V. Belolipov, D. Zaurov, S.W. Eisenman, The Geography, *Climate and Vegetation of Uzbekistan,* Medicinal Plants of Central Asia: Uzbekistan and Kyrgyzstan, ed S W Eisenman, D E Zaurov and L Struwe (New York, NY: Springer New York), 5-7 (2013)
21. J. Gerts, M. Juliev, A. Pulatov, *Multi-temporal monitoring of cotton growth through the vegetation profile classification for Tashkent province, Uzbekistan,* J. GeoScape, **14**, 62-9 (2020)
22. R. Niyazov, B. Nurtaev, *Modern Seismogenic Landslides Caused by the Pamir-Hindu Kush Earthquakes and Their Consequences in Central Asia,* J. Landslide Science and Practice: Volume 5: Complex Environment, ed C Margottini, P Canuti and K Sassa (Berlin, Heidelberg: Springer Berlin Heidelberg), 343-8 (2013)
23. S. K. McFEETERS, *The use of the Normalized Difference Water Index (NDWI) in the delineation of open water features,* Int. J. Remote Sensing**, 17,** 1425-32 (1996)
24. M. Immitzer, C. Atzberger, *Early Detection of Bark Beetle Infestation in Norway Spruce (<I>Picea abies</I>, L.) using WorldView-2,* J. Photogrammetrie - Fernerkundung - Geoinformation, 51-67 (2014)
25. P. Toscani, M. Immitzer, C. Atzberger, *Wavelet-based texture measures for object-based classification of aerial images*, J. pfg, 105-21 (2013)
26. T. Blaschke, B. Feizizadeh, D. Holbling, *Object-Based Image Analysis and Digital Terrain Analysis for Locating Landslides in the Urmia Lake Basin, Iran*, IEEE J. Selected Topics in Applied Earth Observations and Remote Sensing, **7**, 4806-17 (2014)
27. J. Michel, D. Youssefi, M. Grizonnet, *Stable Mean-Shift Algorithm and Its Application to the Segmentation of Arbitrarily Large Remote Sensing Images,* J. IEEE Trans. Geosci. Remote Sensing, **53,** 952-64 (2015)
28. J. Inglada, E. Christophe, *The Orfeo Toolbox remote sensing image processing software*, J. IEEE International Geoscience and Remote Sensing Symposium, 733-6 (2009)
29. W-T. Ng, M. Meroni, M. Immitzer, S. Böck, U. Leonardi, F. Rembold, H. Gadain, C. Atzberger, *Mapping Prosopis spp. with Landsat 8 data in arid environments: Evaluating effectiveness of different methods and temporal imagery selection for Hargeisa, Somaliland,* Int. J. Applied Earth Observation and Geoinformation, **53**, 76-89 (2016)
30. G. M. Foody, *Status of land cover classification accuracy assessment*, J. Remote Sensing of Environment, **80,** 185-201 (2002)
31. K.C. Devkota, A.D. Regmi, H.R. Pourghasemi, K. Yoshida, B. Pradhan, I.C. Ryu, M.R. Dhital, O.F. Althuwaynee, *Landslide susceptibility mapping using certainty factor, index of entropy and logistic regression models in GIS and their comparison at Mugling–Narayanghat road section in Nepal Himalaya,* J. Natural Hazards, **65,** 135-65 (2013)
32. I. Aslanov, K. Sh, O. Sh, A. Jumanov, Z. Jabbarov, I. Jumaniyazov, N. Namozov, *Evaluation of soil salinity level through using Landsat-8 OLI in Central Fergana valley, Uzbekistan,* J. E3S Web of Conferences, **258, (**2021)